



Research Article

Formulation And Evaluation of Transdermal Patches Containing Astragaloside IV

Suhas B. C., Nagendra R.*, Siddartha H. N., Venkatesh, Hanumanthachar Joshi

Sarada Vilas College of Pharmacy, Mysuru, Karnataka, India.

ARTICLE INFO

Published: 27 Oct 2025

Keywords:

Astragaloside IV,
transdermal patch, HPMC,
PVP, sustained release,
topical delivery, drug
release

DOI:

10.5281/zenodo.17452263

ABSTRACT

This research centers on the development and characterization of transdermal patches containing Astragaloside IV, employing hydroxypropyl methylcellulose (HPMC) and polyvinylpyrrolidone (PVP) as the primary polymers. The objective of the study was to design a topical patch system that enhances stability, sustained drug release, skin compatibility, and patient compliance. Multiple patch formulations (F1–F5) were prepared using variable ratios of HPMC and PVP, then systematically evaluated for their physicochemical properties, including organoleptic characteristics, FTIR spectroscopy, microscopic uniformity, thickness, weight, tensile strength, folding endurance, moisture content, drug content, pH, flexibility, and in vitro drug release. Astragaloside IV was confirmed to be a white to off white, odorless crystalline powder with high solubility in methanol, ethanol, and DMSO. UV spectrophotometric analysis established λ_{max} at 256 nm in methanol. FTIR and DSC studies showed no drug–polymer incompatibility. Microscopy revealed smooth, homogeneous films without visible defects. Drug content was consistent across batches (96.9–98.4%), confirming uniform incorporation. The optimized formulation showed cumulative release above 93.25 ± 0.474 after 12 hours, with kinetics fitting first-order and Korsmeyer–Peppas models, indicating diffusion-controlled sustained release. Stability studies confirmed integrity and efficacy under accelerated conditions, demonstrating successful development of stable hydrophilic polymer-based patches for prolonged topical delivery of Astragaloside IV.

INTRODUCTION

The development of novel drug delivery systems is a key focus in pharmaceutical research, aimed at overcoming the limitations of conventional oral

and parenteral routes. Although oral administration is convenient and preferred by patients, it is limited by enzymatic degradation in the gastrointestinal tract, poor absorption, first-pass metabolism, and gastrointestinal irritation.

*Corresponding Author: Nagendra R.

Address: Sarada Vilas College of Pharmacy, Mysuru, Karnataka, India.

Email : bcsuhas50@gmail.com

Relevant conflicts of interest/financial disclosures: The authors declare that the research was conducted in the absence of any commercial or financial relationships that could be construed as a potential conflict of interest.



These issues often necessitate higher or more frequent dosing, reducing therapeutic efficacy and increasing side effects. Parenteral delivery bypasses first-pass metabolism and provides rapid action but is invasive, painful, and associated with infection risk and poor compliance, particularly in paediatric and geriatric patients.¹ Transdermal Drug Delivery Systems (TDDS) have emerged as a promising alternative. They offer controlled and sustained drug release, avoidance of hepatic metabolism, reduced dosing frequency, and improved adherence. While the concept originated in traditional medicine through medicated plasters, modern TDDS have evolved into advanced, patient-friendly systems. However, the skin—especially the stratum corneum—poses a significant barrier. Only drugs with favourable physicochemical properties, such as low molecular weight and balanced lipophilicity, can permeate effectively. To enhance penetration, permeation enhancers and novel carrier systems are often

employed.¹ Recent advancements have improved the feasibility of TDDS, with more than 20 patches approved worldwide for conditions such as pain, hormonal imbalance, and cardiovascular diseases. Nearly 40% of new drug candidates are now exploring dermal or transdermal routes, highlighting their growing importance. TDDS may act locally (dermal) or systemically, the latter providing controlled delivery into systemic circulation while remaining non-invasive.¹ In conclusion, TDDS represent a rapidly advancing approach that can improve therapeutic outcomes by enhancing efficacy, safety, and patient compliance. This thesis focuses on formulation strategies, permeability challenges, and recent technological innovations in TDDS. Greater understanding of skin–drug interactions and integration of nanotechnology are expected to further expand their clinical potential in the near future.²

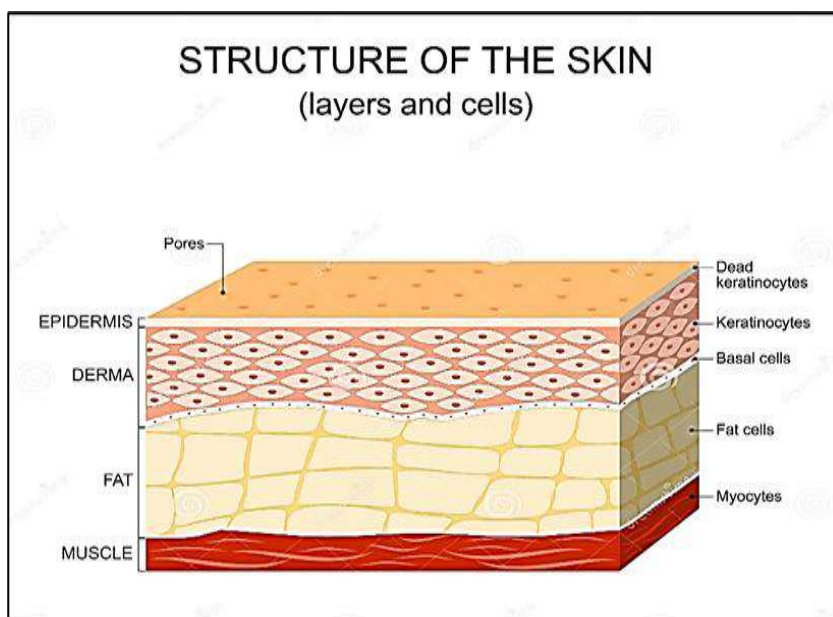


Figure 1: Structure Of Skin²

Skin as a Site of Percutaneous Absorption

Human skin, covering nearly 2 m² in adults, is composed of three primary layers: the epidermis, dermis, and subcutaneous tissue. The outermost

layer of the epidermis, the stratum corneum (SC), is only 10–20 µm thick but represents the major barrier to percutaneous absorption. It consists of keratin-filled, flattened corneocytes embedded in a lipid matrix arranged in alternating hydrophilic

and lipophilic lamellae. This “brick-and-mortar” structure effectively restricts the penetration of most xenobiotics. The viable epidermis beneath is more permeable but lacks vasculature, receiving nutrients by diffusion from the dermal capillaries.

The dermis, rich in blood vessels and connective tissue, represents the site of systemic absorption, while the underlying subcutaneous tissue provides cushioning and thermal regulation.³

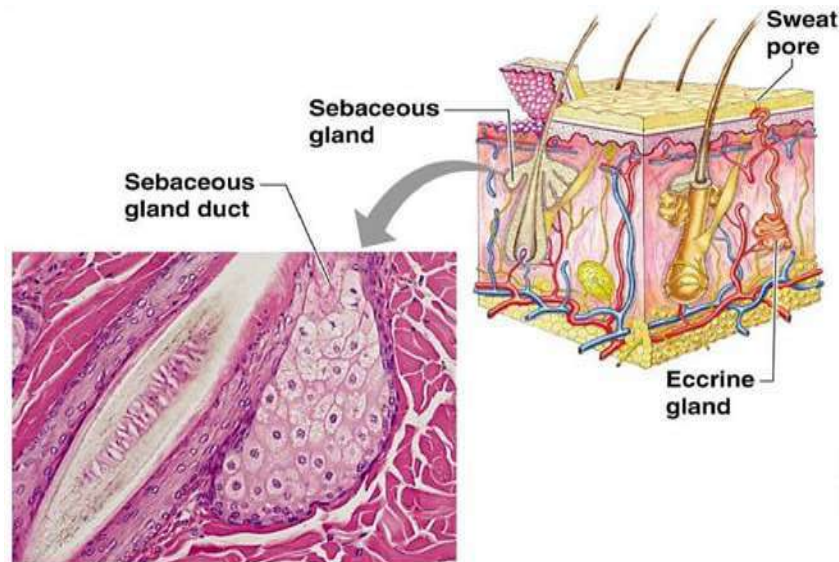


Figure 2: Skin appendages and their associated structures

Drug molecules can traverse the skin by three main pathways: (i) the transcellular route through corneocytes, favouring hydrophilic molecules; (ii) the intercellular lipid route, favouring lipophilic compounds; and (iii) appendageal pathways through hair follicles and sweat glands, which represent only ~0.1% of the surface but can provide entry sites for ions, macromolecules, or

particulate carriers. However, the SC barrier remains the dominant determinant of absorption, and most drug candidates fail to reach therapeutic systemic levels without additional formulation strategies.⁴

Mechanism Of Percutaneous Penetration⁴

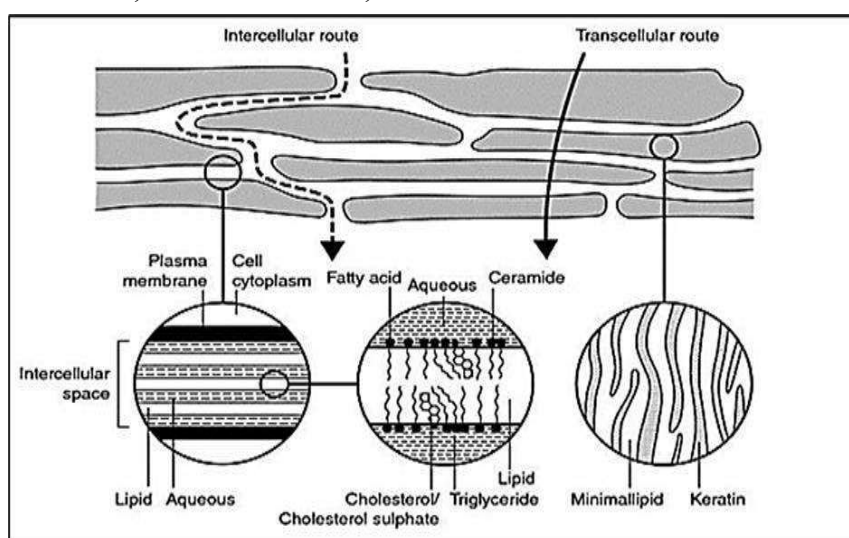


Figure 3: Simplified diagram of stratum corneum and two micro-routes of drug penetration

2. Aim And Objective:

A) Aim:

To design, optimize, and evaluate a safe, stable, and patient-friendly transdermal drug delivery system (TDDS) of Astragaloside IV

B) Objectives Of the Study:

The present work is undertaken with the following objectives:

TABLE I. Preformulation Studies

TABLE II. Formulation Development

TABLE III. Physicochemical Evaluation of Patches

TABLE IV. In Vitro Performance Testing

TABLE V. Stability Assessment

3. MATERIALS AND METHODS

A) MATERIALS

Astragaloside IV was obtained from Dham Tec Pharm and Consultant (Mumbai, India). Hydroxypropyl methylcellulose (HPMC) was purchased from Otto Chemika-Biochemical Reagents (Mumbai, India). Polyvinylpyrrolidone K30 (PVP K30), polyethylene glycol (PEG), oleic acid, and glycerine were supplied by Karnataka Fine Chemicals (Bangalore, India). Ethanol was procured from Bio Liqua Research Pvt. Ltd. (Bangalore, India).

B) METHODOLOGY

Preformulation studies

Preformulation studies are critical in the development of a transdermal drug delivery system (TDDS). They provide information on the

physicochemical properties of the drug, excipient compatibility, and suitability for incorporation into the patch matrix. The following parameters are typically evaluated⁷

Organoleptic properties

Astragaloside IV's organoleptic properties, including appearance, colour, and odour, were characterized using descriptive methods; taste assessment was not performed due to API safety policy.⁷

Determination of melting point

"A small quantity of Astragaloside IV was introduced into a capillary tube sealed at one end and placed in a melting point apparatus. The temperature at which the sample softened and decomposed was carefully recorded. The procedure was repeated three times, and the average decomposition/melting point was reported.⁸

Solubility Analysis⁹

Astragaloside IV's solubility will be tested in various solvents, including water, methanol, ethanol, propylene glycol, PEG-400, and DMSO.

Calibration Curve of Astragaloside IV¹⁰⁻¹²

A calibration curve of Astragaloside IV was constructed using the UV-visible spectrophotometric method. Precisely 50 mg of Astragaloside IV was weighed and transferred into a 50.0 mL volumetric flask, dissolved in HPLC-grade methanol, and diluted to volume to obtain a stock solution of 1000 $\mu\text{g}\cdot\text{mL}^{-1}$. The stock solution was stored at 2–8 °C and protected from light. The UV spectrum of the stock solution was scanned between 200 and 800 nm using a Shimadzu UV-2450 spectrophotometer. The Maximum absorption wavelength (λ_{max}) was identified.



From the stock, working standard solutions of 5, 10, 15, 20 and 25 $\mu\text{g}\cdot\text{mL}^{-1}$ were prepared from the stock by appropriate dilution in methanol; all solutions were filtered through 0.22 μm syringe filters prior to measurement. The absorbance of each standard (measured in triplicate) was recorded at 256 nm versus a methanol blank. A calibration curve was constructed by plotting concentration ($\mu\text{g}\cdot\text{mL}^{-1}$) on the X-axis against mean absorbance on the Y-axis.

Drug-excipient compatibility studies by FTIR. 13-17

The drug-polymer and polymer-polymer interactions of Astragaloside IV were investigated using an FTIR spectrometer. Approximately 100 mg of dried potassium bromide (KBr) was added after the drug and polymer were finely ground and blended together in a mortar and pestle to ensure uniform mixing. The mixture was then compressed into a transparent disc using an evacuable die under high pressure. A hydraulic press can also be employed as a simpler alternative to prepare suitable KBr pellets. Baseline correction was carried out using pure, dried KBr. Finally, the prepared drug KBr discs were scanned in the spectral range of 4000–400 cm^{-1} to identify possible interactions.

Differential Scanning Calorimetry¹⁸

DSC studies of pure Astragaloside IV were performed. Precisely weighed samples were

placed in DSC aluminium pans, and heating curves were recorded over a temperature range of 40–350 °C at a heating rate of 10 °C/min under an inert nitrogen atmosphere. The DSC thermograms were obtained using calibrated differential scanning calorimeters to analyse phase transitions and confirm drug purity and thermal stability.

Formulation of transdermal patches of Astragaloside IV¹⁹⁻²³

The transdermal patches of Astragaloside IV were prepared by the solvent-casting technique. As shown in Table 3, polymeric films were formulated using hydroxypropyl methylcellulose (HPMC) and polyvinylpyrrolidone (PVP) in varying ratios, maintaining a total polymer weight of 300 mg. The polymers were dissolved in ethanol: water (80:20 v/v) under magnetic stirring, and polyethylene glycol 400 (30% w/w of total polymer weight) was added as a plasticizer. Astragaloside IV (15 mg/patch), pre-dissolved in a small quantity of ethanol or DMSO, was incorporated into the polymeric solution with gentle stirring for 10 minutes. The mixture was cast onto clean polyester backing films fixed in Petri plates, covered with inverted funnels, and dried overnight at room temperature. Dried patches were peeled off, inspected for uniformity, cut to the desired size, and stored in a desiccator until further evaluation.

Table 1: Composition of Transdermal patches of Astragaloside IV

Ingredients	Formulation code				
	F1	F2	F3	F4	F5
Astragaloside IV (mg)	15	15	15	15	15
HPMC (mg)	250	235	220	185	170
PVP (mg)	50	65	80	115	130
PEG 400 (ml)	2	2	2	2	2
Oleic Acid(ml)	1	1	1	1	1
Ethanol: water	12	12	12	12	12



4. Evaluation of Transdermal patches of Astragaloside IV:

Physical appearance ²⁴

The colour, clarity, flexibility, and smoothness of each prepared transdermal patch were evaluated.

Thickness of the patch ²⁴

Using a screw gauge, three distinct patch thicknesses were measured, and mean values were calculated.

Weight Uniformity ²⁴

The patches measuring $1 \times 1 \text{ cm}^2$ were cut and weighed using an electronic balance. The average weight was calculated and recorded.

Tensile strength ²¹

The tensile strength of the patches was evaluated using a Universal Strength Testing Machine with a sensitivity of 1 gram. The instrument was equipped with two load cell grips, in which the lower grip remained fixed while the upper grip was movable. A test film of dimensions $4 \times 1 \text{ cm}^2$ was placed between the grips, and a gradually increasing force was applied until the film ruptured. The tensile strength of the film was then determined from the kilogram dial reading. Tensile strength is expressed as follows.

Folding endurance ²⁰

Folding endurance of the prepared films was evaluated manually. A strip of film ($5 \times 5 \text{ cm}$) was repeatedly folded at the same position until it broke. The total number of folds a film could withstand at the same spot without breaking or cracking was recorded as its folding endurance.

Percentage moisture absorption ²⁰

The patches were accurately weighed and placed in a desiccator containing saturated potassium chloride solution, maintained at room temperature to provide 80–90% relative humidity. They were stored until a constant weight was obtained, after which the patches were removed and reweighed. The percentage of moisture uptake was calculated from the difference between the initial and final weights, relative to the initial weight.

Percentage moisture loss ²³

The patches were individually weighed and placed in a desiccator containing anhydrous calcium chloride at room temperature. Once a constant weight was achieved, the final weight was noted. The percentage of moisture loss was calculated by comparing the difference between the initial and final weights with respect to the initial weight.

Drug Content ²⁵

A patch of 1 cm^2 was accurately cut and placed in a 50 mL volumetric flask containing 10 mL of phosphate buffer (pH 7.4). The dispersion was stirred continuously for 4h and then kept undisturbed overnight to ensure complete extraction of the drug from the patch. The absorbance of the obtained solution was recorded at 256 nm using a UV–Visible spectrophotometer, with the respective buffer used as blank. To ensure reproducibility and reliability, the procedure was repeated five times.

In-vitro drug release kinetics ²⁵

The *in vitro* drug release kinetics of the formulated transdermal patches were analyzed by fitting the release data to different mathematical models, namely zero-order, first-order, Higuchi, and Korsmeyer–Peppas equations, to determine the predominant release mechanism of Astragaloside



IV. The zero-order model describes a constant rate of drug release independent of concentration, expressed as $Q = Q_0 + K_0 t$, which is ideal for maintaining uniform drug levels and ensuring sustained therapeutic efficacy. The first-order model, represented by $\log C = \log C_0 - Kt/2.303$, indicates that the release rate is proportional to the remaining drug content, leading to a gradual decline in release over time. The Higuchi model ($Q = Kt^{1/2}$) explains diffusion-controlled release from a polymeric matrix, where the drug diffuses through the matrix according to Fick's law. The Korsmeyer–Peppas model ($M_t/M_\infty = Kt^n$) is an empirical equation that helps to elucidate both Fickian and anomalous transport mechanisms, with the release exponent (n) providing insights into the nature of diffusion. For each formulation, the correlation coefficient (R^2) and release rate constant (k) were calculated, and the model with the highest R^2 value was considered the best fit, offering a better

understanding of the drug release behaviour and mechanism from the Astragaloside IV transdermal patches.

Stability Studies ²⁶

The stability of the prepared Astragaloside IV transdermal patches was evaluated under accelerated storage conditions to assess their reliability and predict long-term performance. To protect them from light, air, and moisture, the patches were sealed in laminated aluminium foil pouches. As per ICH guidelines, samples were stored at 40 ± 2 °C and $75 \pm 5\%$ RH for three months, with evaluations carried out at predetermined intervals—Day 0, Day 15, 1 month, 2 months, and 3 months.

5. RESULTS AND DISCUSSION

a) Preformulation studies

Organoleptic properties

Table 2: Organoleptic Properties of Astragaloside IV

Sl. No.	Parameter	Specification	Results
1.	Colour	White to off-white	Complies
2.	Odour	Odourless	Complies
3.	Taste	Slightly bitter	Complies
4.	Appearance	Crystalline powder	Complies

Melting point of Astragaloside IV

The reported melting point of Astragaloside IV was found by the capillary technique to be 245 – 254°C

Solubility Analysis

The solubility of the drug was assessed in various solvents to identify a suitable medium capable of dissolving both the drug and the excipients used in formulation. Factors such as pH, ionic strength, temperature, and buffer concentration are known to influence the solubility of a drug. The results are shown in the table number 3.

Table 3: Solubility data of Astragaloside IV

Sl. No.	Solvent	Solubility
1	Methanol	Very soluble
2	Ethanol	Very soluble
3	Ethyl acetate	Slightly soluble
4	Dimethyl Sulfoxide.	Freely soluble



5	Chloroform	Slightly soluble
6	Water	Very slightly soluble

Calibration Curve of Astragaloside IV

The maximum absorption of the Astragaloside IV solution, which was scanned between 200 to 800

nm, occurred at 256 nm. Utilizing a UV-visible spectrophotometer, the absorbance of the prepared solution was measured at 256 nm.

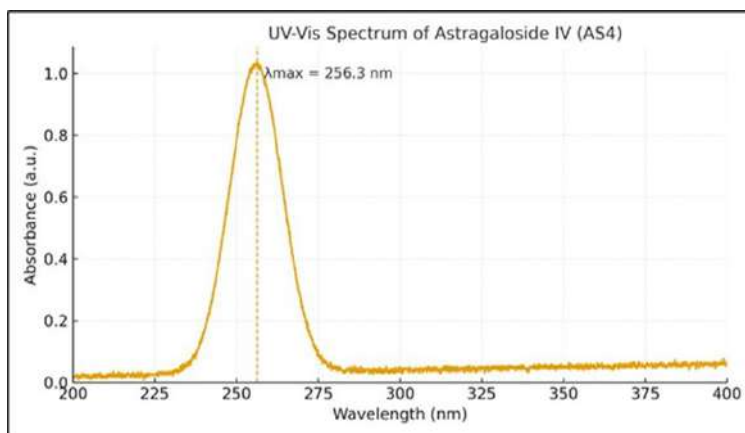


Figure 4: Absorption maxima of Astragaloside IV

The wavelength of maximum absorption (λ_{max}) in methanol was found to be 256.3 nm.

Table 4: Data for calibration Curve of Astragaloside IV in Methanol

Sl. No.	Concentration($\mu\text{g/mL}$)	Absorbance ($\lambda = 256 \text{ nm}$)
1.	0	0.000
2.	5	0.161
3.	10	0.321
4.	15	0.481
5.	20	0.641
6.	25	0.801

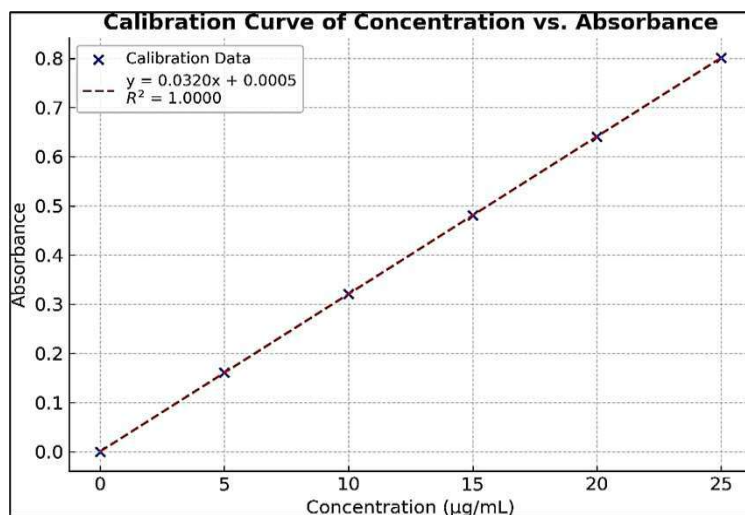


Figure 5: Calibration Curve of Astragaloside IV

The maximum absorption (λ_{max}) of Astragaloside IV in methanol was observed at 256 nm. Its depiction in the figure number 7. A calibration curve was constructed by plotting absorbance versus concentration. The regression equation was found to be $y = 0.0320x + 0.0005$, with a

correlation coefficient ($r^2 = 1.0000$), indicating perfect linearity and confirming the method's reliability for quantitative analysis. The results are shown in the figure number 5 and table number 4.

Drug-excipient compatibility studies by FTIR

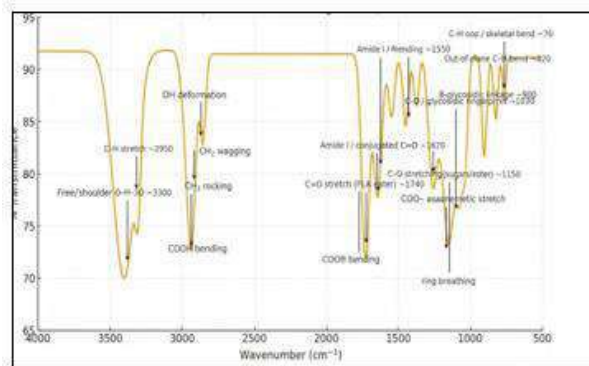


Figure 6: FTIR Spectrum of Astragaloside IV

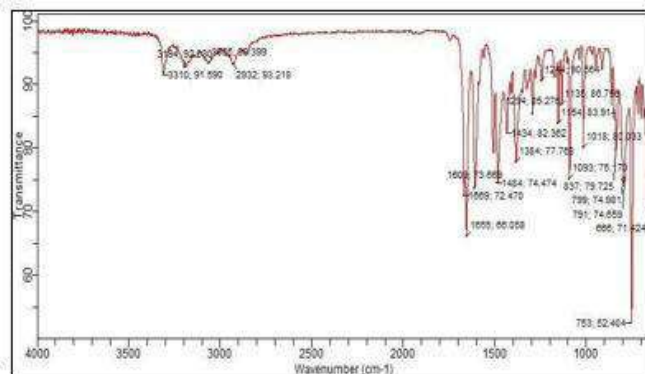


Figure 7: FTIR Spectrum of HP

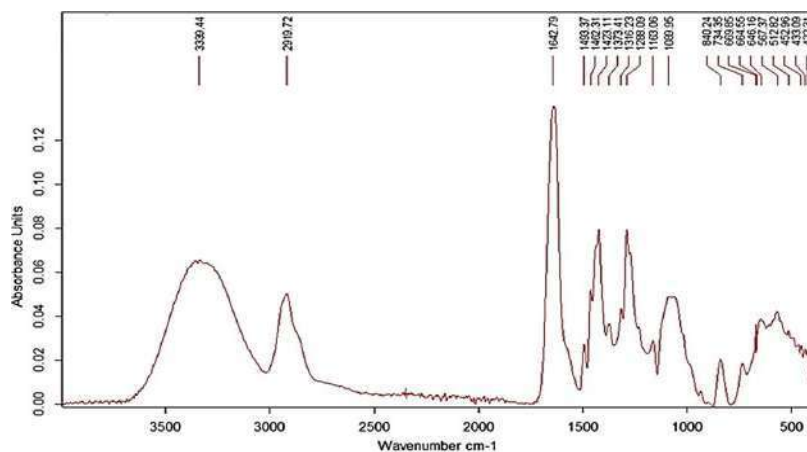


Figure 8: FTIR Spectrum of Polyvinylpyrrolidone k 30

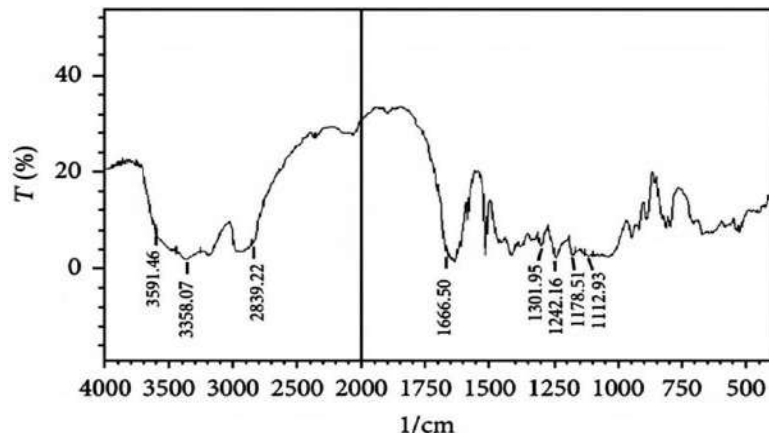


Figure 9: FTIR spectrum of physical mixture of Astragaloside IV

Table 5: FTIR Peaks of Astragaloside IV

Reference Peaks (cm-1)	Obtained Peaks (cm-1)	Functional Groups
3400–3200	3375.24	O–H stretching
2940–2850	2925.18	C–H stretching
1725–1700	1712.38	C=O stretching
1670–1600	1635.42	C=C bending
1450–1375	1384.26	C–O–C stretching
1250–1050	1076.58	C–H bending
900–750	861.58	Anomeric region

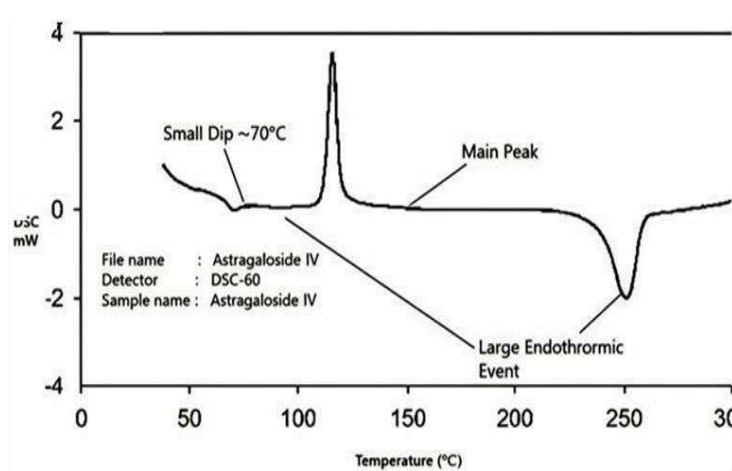
Table 6: Comparative FTIR spectral data of drug and excipients

Obtained peaks (cm-1)	Obtained peaks (cm-1) of physical mixture	Functional groups
3375.24	3591.46	O–H stretching
2925.18	3358.07	C–H stretching
1712.38	2839.22	C=O stretching
1635.42	1666.50	C=C bending
1384.26	1301.95	C–O–C stretching
1076.58	1242.16	C–H bending
861.58	889.26	Anomeric region

The peaks observed in the FTIR spectra correspond to the characteristic functional groups of Astragaloside IV, confirming the identity of the drug. Both the FTIR spectra of pure Astragaloside IV and the physical mixture with polymers show similar peak patterns and positions. The physical mixture's FTIR peaks remain consistent with those of the pure drug, indicating that there is no

significant interaction between Astragaloside IV and the polymers used. This confirms the compatibility and physical mixing of the drug with the polymer matrix without chemical modification.

Differential Scanning Calorimetry of Astragaloside IV

**Fig 10: Differential Scanning Calorimetry of Astragaloside IV**

The purity and compatibility of Astragaloside IV were evaluated using differential scanning calorimetry (DSC). The DSC thermogram of the

pure drug exhibited a sharp and well-defined endothermic peak at around 250 °C, corresponding to its melting point. This sharp melting peak

confirms the crystalline nature and thermal stability of Astragaloside IV in its pure form. When the drug was analysed in physical mixtures with the selected polymers, a similar endothermic peak appeared at nearly the same temperature (~ 250 °C). The retention of this characteristic peak in the thermograms of the mixtures indicates that there was no significant drug–polymer interactions, since any strong interaction or incompatibility would have caused noticeable shifts, broadening, or disappearance of the peak. Thus, the DSC analysis not only confirms the purity of Astragaloside IV but also demonstrates that its crystalline characteristics are preserved in

the formulation. This suggests that the drug remains stable and compatible with the chosen excipients, making it suitable for further formulation development.

B) Evaluation of Transdermal patches of Astragaloside IV

Physical appearance

The Astragaloside IV formulated patches were observed to be clear, smooth, uniform, and flexible in their physical appearance, without any entrapment of air bubbles or cracks.

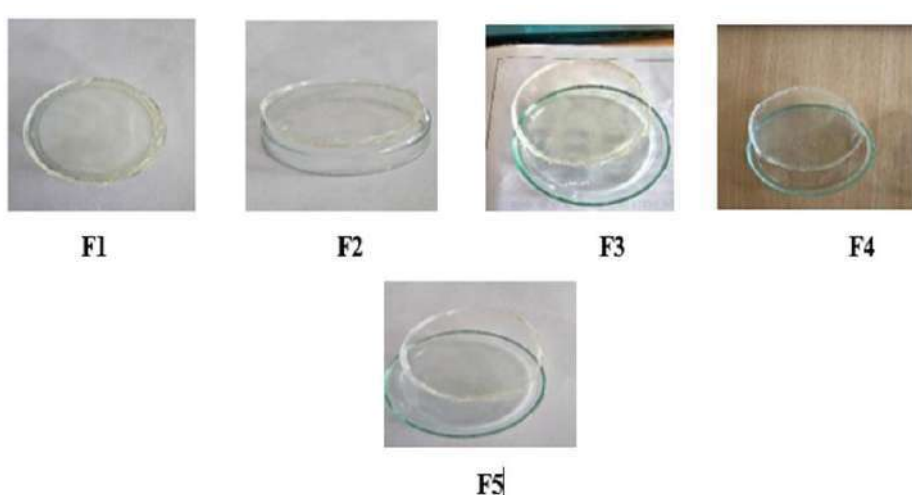


Figure 11: F1 to F5 Formulation of Transdermal patches of Astragaloside IV

Uniformity of weight

The uniformity of weight of the prepared Astragaloside IV patches was evaluated, and the data are shown in figure number 12. The average weight of patches was found in the range of 399.27

± 0.80 to 402.90 ± 0.36 mg, with low standard deviation values indicating uniformity of the process. The results confirm that the prepared patches complied with the uniformity of weight requirement, showing good reproducibility in formulation.

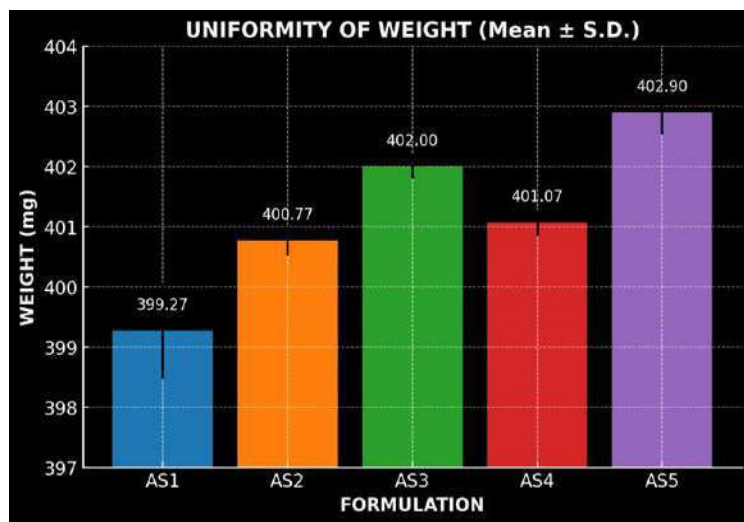


Figure 12: Graphical representation of Uniformity of Weight

Thickness of the patch

The prepared transdermal patches exhibited consistent thickness across all formulations, ranging from 0.18 ± 0.006 mm to 0.22 ± 0.006 mm. This uniformity in thickness indicates a

controlled and reproducible fabrication process, essential for ensuring consistent drug release and optimal performance of the patches in transdermal drug delivery applications. The results obtained were depicted in figure 13.

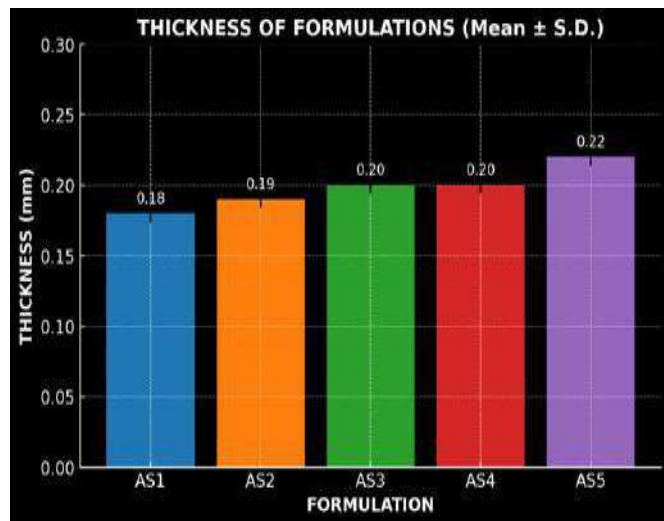


Figure 13: Graph of Thickness

Tensile Strength

The tensile strength of the Astragaloside IV transdermal patches reflected their ability to resist rupture. The patches showed good tensile strength, ranging from 0.42 ± 0.012 to 0.59 ± 0.014 kg/cm², attributed to the presence of PEG 400 as a plasticizer. No cracking was observed, confirming

adequate flexibility and mechanical stability. Percentage elongation, measured using a Hounsfield universal testing machine, indicated satisfactory stretchability before breaking. The order of tensile strength was AS5 > AS4 > AS2 > AS3 > AS1, while percentage elongation followed the order AS5 > AS3 > AS4 > AS2 > AS1. The result is shown in figure number 14.

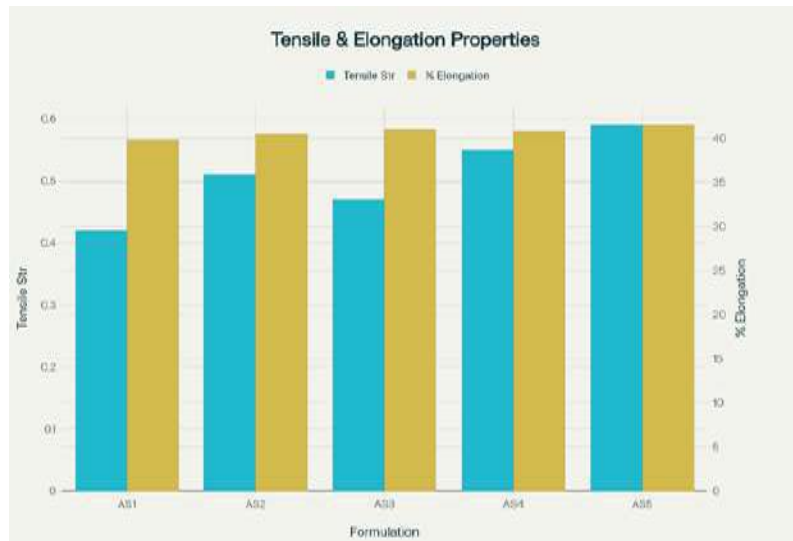


Figure 14: Graph of Tensile Strength

Folding endurance

The folding endurance values of the prepared Astragaloside IV patches varied between 180 ± 2.0 to 260 ± 2.0 folds (Table 13). The formulated film AS5 exhibited optimal folding endurance (260

folds) without any significant batch variation. The results were found satisfactory, indicating that the patches would not break and would maintain their integrity during handling and application. The results are depicted in the figure 15.

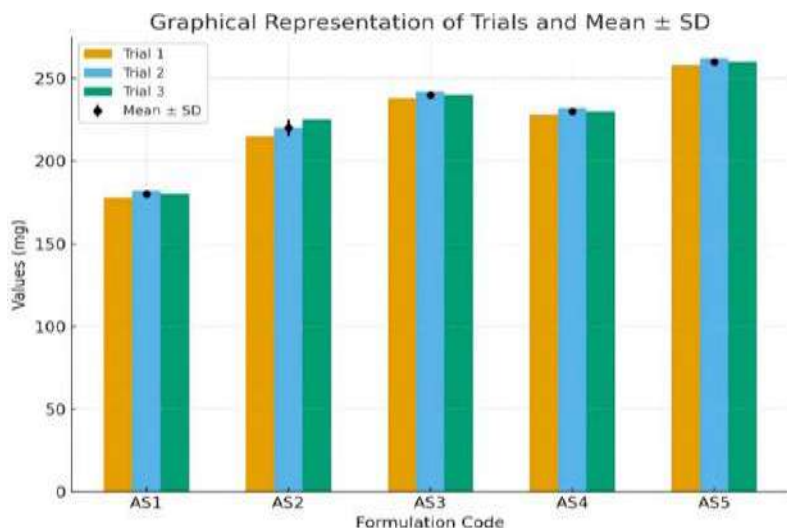


Figure 15: Graphical depiction of Folding endurance

Percentage moisture absorption

The percent moisture absorption values of the prepared Astragaloside IV patches are shown in figure number 19, and the order of percentage moisture absorption was found to be AS5 > AS4

> AS3 > AS2 > AS1. The values varied between $2.15 \pm 0.08\%$ and $4.85 \pm 0.15\%$. This indicates that the patches absorbed only a small amount of atmospheric moisture, which is desirable to maintain flexibility and prevent brittleness. The results confirm that all the prepared patches

possess satisfactory stability and mechanical integrity under normal storage conditions and the

result are graphically represented in the figure number 16.

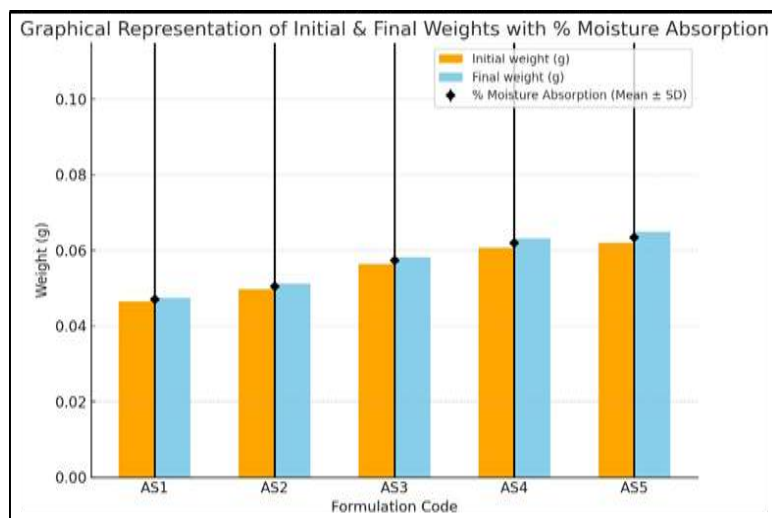


Figure 16: Graph of Percentage moisture absorption

Percentage moisture loss

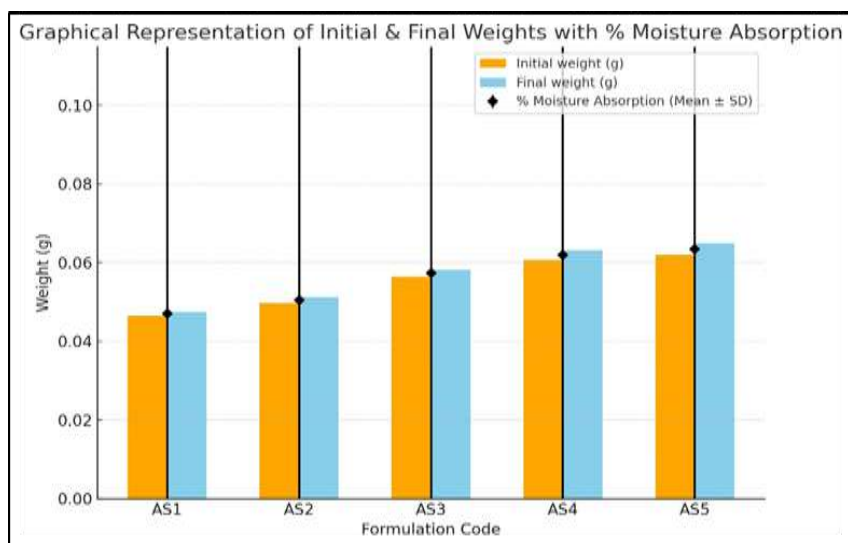


Figure 17: Graph of Percentage moisture loss

The studies on moisture loss were conducted at 80–90% relative humidity. All of the Astragaloside IV patches exhibited minimal percentage of moisture loss. The data is presented in figure 17, with the percentage moisture loss occurring in the following order: AS2 > AS5 > AS4 > AS1 > AS3. The low moisture content of the formulations helps maintain their stability and

prevents the films from drying out completely or becoming brittle.

Drug content

Data of Astragaloside IV estimation in transdermal patches by UV-visible spectrophotometer at 256 nm have been recorded and graphically represented in figure number 18. The formulation's percentage drug content ranges from 96.9 ± 0.3 to

98.4 ± 0.3 . The low standard deviation values indicate uniform drug distribution within the

polymeric matrix, confirming reproducibility of the manufacturing process.

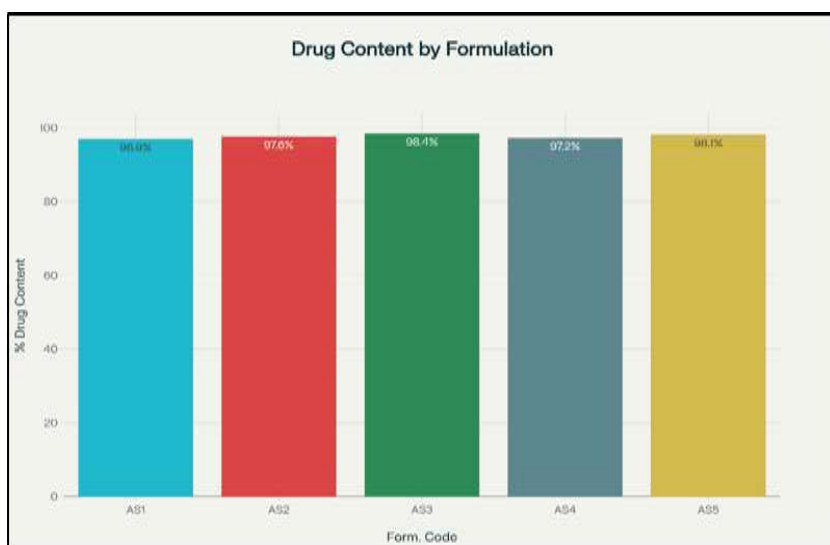


Figure 18: Graphical representation of Drug content

In-vitro release studies

Table 7: Percentage Cumulative Drug Release

Time (min)	% Cumulative Drug Release (Mean \pm S.D.) *				
	Formulation Code				
	AS 1	AS 2	AS 3	AS 4	AS 5
0	0	0	0	0	0
15	8.42 ± 0.215	12.36 ± 0.352	10.25 ± 0.295	9.58 ± 0.187	11.21 ± 0.246
30	14.85 ± 0.318	20.54 ± 0.447	18.33 ± 0.321	15.92 ± 0.264	17.65 ± 0.382
60	28.67 ± 0.428	34.72 ± 0.518	32.45 ± 0.411	29.38 ± 0.333	30.82 ± 0.401
120	42.15 ± 0.462	50.16 ± 0.612	48.39 ± 0.503	44.73 ± 0.426	46.95 ± 0.512
240	56.82 ± 0.573	65.27 ± 0.437	62.84 ± 0.389	58.12 ± 0.357	61.48 ± 0.469
360	69.38 ± 0.421	78.41 ± 0.583	75.26 ± 0.528	71.45 ± 0.441	73.92 ± 0.517
480	80.46 ± 0.533	85.63 ± 0.391	83.72 ± 0.612	82.11 ± 0.518	84.35 ± 0.449
600	86.23 ± 0.412	89.74 ± 0.523	89.74 ± 0.523	87.15 ± 0.482	88.65 ± 0.493
720	90.18 ± 0.532	93.25 ± 0.474	92.08 ± 0.513	91.36 ± 0.437	92.79 ± 0.521

* All values represent the mean of 3 readings (n-3)

The cumulative percentage of drug released over 12 h ranged from 90.18 ± 0.532 % (AS1) to 93.25 ± 0.474 % (AS2) for the Astragaloside IV transdermal films.

The order of drug release among the formulations was:

AS2 > AS5 > AS3 > AS4 > AS1.

The formulation AS2 showed a better in-vitro drug release profile across the cellulose membrane when compared to the other formulations. This might be attributed to the suitable combination of polymers, plasticizer concentration, and the effect of permeation enhancer used. Thus, formulation AS2 is considered the optimized formulation. The results are depicted in Table number 7 and figure 19.

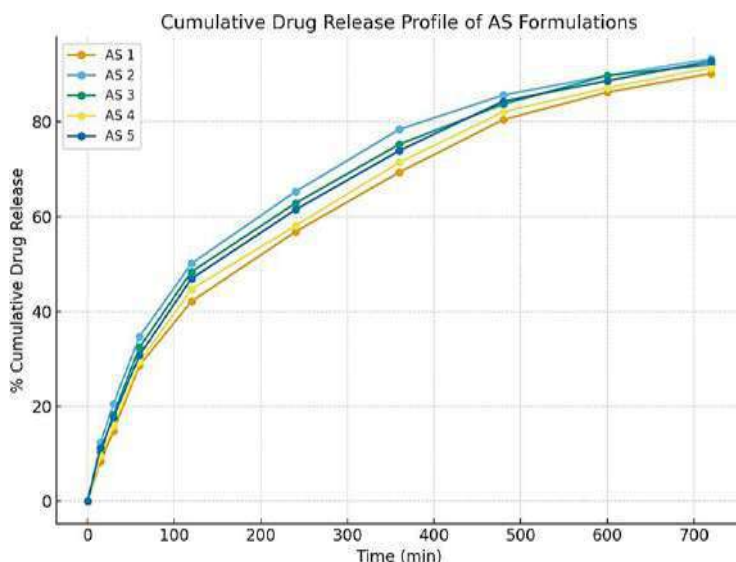


Figure 19: Cumulative Drug Release Profile

Drug Release Kinetics

The cumulative percentage of Astragaloside IV released from the AS2 formulation was analyzed by fitting the data into various mathematical kinetic models, including zero-order, first-order, Higuchi, and Korsmeyer–Peppas models, in order to elucidate the mechanism of drug release. The correlation coefficients (R^2) obtained from these models were used to determine the best-fit model that most accurately described the release behaviour. The selection of the most appropriate kinetic model was based on the highest regression coefficient (R^2) value, as an R^2 value approaching unity indicates a strong linear relationship and a better model fit. For the AS2 formulation, the first-order model exhibited the highest R^2 value ($R^2 = 0.995$), suggesting that the release of Astragaloside IV from the patch follows a concentration-dependent kinetic profile. This implies that the rate of drug release decreases exponentially with time, as the concentration of the drug in the matrix diminishes a typical behavior for diffusion-controlled systems where the driving force for release is the concentration gradient between the patch and the skin surface. In addition, the AS2 formulation also showed relatively high correlation values for the Higuchi model ($R^2 =$

0.977) and the Korsmeyer–Peppas model ($R^2 = 0.973$). The Higuchi model describes drug release from a homogenous matrix as a function of the square root of time, which is indicative of Fickian diffusion. The strong fit to this model further supports that the release mechanism is primarily diffusion-controlled, governed by the gradual penetration of the dissolution medium into the polymeric network and subsequent release of the drug molecules along the concentration gradient. Furthermore, the Korsmeyer–Peppas model was applied to evaluate the mechanism of drug release in more detail. The release exponent (n) obtained from this model helps to distinguish between Fickian diffusion, non-Fickian (anomalous) transport, or case-II transport. For the AS2 formulation, the n value (typically between 0.45 and 0.89 for polymeric films) indicated anomalous diffusion, suggesting that both diffusion and polymer relaxation (erosion/swelling) contribute to the overall release process. This hybrid mechanism is characteristic of hydrophilic polymeric systems containing HPMC and PVP, where water uptake induces swelling, creating additional pathways for the drug to diffuse through the matrix. Overall, these findings suggest that the *in vitro* release profile of Astragaloside IV from

the AS2 transdermal patch follows first-order kinetics, with a predominant diffusion-controlled release mechanism influenced by the swelling behavior of the polymeric matrix. The high R^2 values across multiple models also indicate that the AS2 formulation provides a consistent and sustained release pattern, which is desirable for maintaining prolonged therapeutic levels of Astragaloside IV through transdermal administration. The corresponding graphical plots

for each kinetic model — including cumulative % drug released vs. time (zero-order), log cumulative % drug remaining vs. time (first-order), cumulative % drug released vs. square root of time (Higuchi model), and log cumulative % drug released vs. log time (Korsmeyer–Peppas model) — are presented in Figures 20-23, respectively, to visually demonstrate the goodness of fit for each kinetic model.



Figure 20: Zero order plot of AS2 formulation

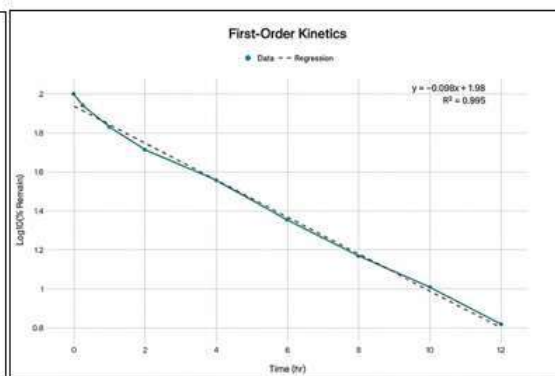


Figure 21: First order plot of AS2 formulation

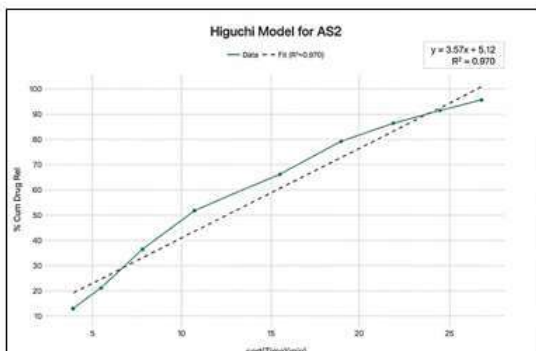


Figure 22: Higuchi Model for AS2 Formulation

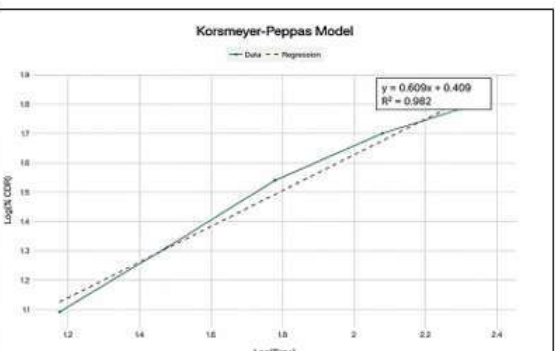


Figure 23: Korsmeyer-peppas model

Stability studies

Formulation Astragaloside IV (F2) transdermal patch successfully passed the stability studies, showing no significant changes in physical

appearance, thickness, weight uniformity, folding endurance, moisture content, moisture uptake, drug content, flatness, tensile strength, percentage elongation, or in vitro drug release profile. The detailed stability study data for formulation AS4 (AS2) are presented in Table number 8.

Table 8: Data of stability studies for F2 formulation

Formulation	Time (Days)	Physical Appearance	Thickness (mm)	Weight (mg)	Folding Endurance	Drug Content (%)	In vitro Drug Release (%)
AS2	Day 1	No phase separation	0.19±0.007	400.77±0.30	220±6	97.6±0.3	93.25±0.52

	After 90 days	No phase separation	0.20±0.009	400.30±0.35	215±8	97.0±0.4	92.80±0.60
--	---------------	---------------------	------------	-------------	-------	----------	------------

CONCLUSION

The present research aimed to formulate and characterize a controlled-release transdermal patch of Astragaloside IV, a bioactive saponin with poor oral bioavailability due to extensive first-pass metabolism and low solubility. Transdermal delivery was selected to enhance systemic availability and provide sustained release of approximately 15 mg/day. Preformulation studies confirmed that Astragaloside IV is a white to off-white crystalline powder, freely soluble in methanol, ethanol, DMSO, and isopropyl myristate, but practically insoluble in water. FT-IR analysis confirmed compatibility between the drug and polymers (HPMC and PVP), indicating no significant interactions. A UV spectrophotometric method at 256 nm showed good linearity ($R^2 \approx 1.0$) within 2-10 $\mu\text{g}/\text{ml}$ and was used for all analytical estimations. Five formulations (AS1-AS5) were prepared by the solvent-casting method using HPMC and PVP in varying ratios, PEG 400 as plasticizer, and DMSO as permeation enhancer. The resulting patches were transparent, smooth, flexible, and uniform in thickness and weight, demonstrating good reproducibility. Folding endurance tests confirmed mechanical strength, while moisture studies showed that PVP-based films absorbed more moisture due to their hygroscopic nature. Drug content uniformity ranged between 95–104%, indicating consistent drug distribution. In-vitro release studies using Franz diffusion cells in phosphate buffer (pH 7.4) revealed sustained drug release for 12 hours, with formulation AS2 showing optimal performance (92.3% release in 12 h) and following first-order kinetics ($R^2 = 0.994$), suggesting an anomalous

diffusion mechanism involving both diffusion and polymer relaxation. Stability studies conducted for 3 months at room temperature confirmed that AS2 maintained its physical integrity, drug content, and release characteristics within acceptable limits. Overall, the study successfully developed a stable, flexible, and uniform transdermal patch capable of delivering Astragaloside IV in a controlled manner, effectively overcoming its oral bioavailability challenges and offering a promising alternative route for sustained therapeutic delivery.

ACKNOWLEDGEMENT

I sincerely thank Sarada Vilas College of Pharmacy, Mysuru, for their invaluable support and providing excellent facilities throughout this research project. The conducive academic environment, continuous encouragement, and provision of necessary resources played a crucial role in the successful completion of this work.

REFERENCES

1. Williams AC, Barry BW. Penetration enhancers. *Adv Drug Deliv Rev.* 2012 Dec 1; 64:128-37.
2. Ramesh P. Transdermal delivery of drugs. *Indian J Pharmacol.* 1997 May 1;29(3):140.
3. Singh A, Bali A. Formulation and characterization of transdermal patches for controlled delivery of Duloxetine Hydrochloride. *J Anal Sci Technol.* 2016 Dec;7(1):1-3.
4. Cleary GW, Beskar E. Transdermal and transdermal-like delivery system

- opportunities. *Bus Brief Pharmatech.* 2004;1-4.
5. Benson HA. Transdermal drug delivery: penetration enhancement techniques. *Curr Drug Deliv.* 2005 Jan 1;2(1):23-33.
6. Kanikkannan N, Kandimalla K, Lamba SS, Singh M. Structure-activity relationship of chemical penetration enhancers in transdermal drug delivery. *Curr Med Chem.* 2000 Jun 1;7(6):593-608.
7. Barry BW. Drug delivery routes in skin: a novel approach. *Adv Drug Deliv Rev.* 2002 Nov 1;54 Suppl 1: S31-40.
8. Hadgraft J. Skin deep. *Eur J Pharm Biopharm.* 2004 Sep 1;58(2):291-9.
9. Barry BW. Novel mechanisms and devices to enable successful transdermal drug delivery. *Eur J Pharm Sci.* 2001 Sep 1;14(2):101-14.
10. Gannu R, Vamshi Vishnu Y, Kishan V, Madhusudan Rao Y. Development of Nitrendipine transdermal patches: in vitro and ex vivo characterization. *Curr Drug Deliv.* 2007 Jan 1;4(1):69-76.
11. Zhan X, Tang G, Chen S, Mao Z. A new copolymer membrane controlling Clonidine linear release in a transdermal drug delivery system. *Int J Pharm.* 2006 Sep 28;322(1 2):1-5.
12. Aqil M, Sultana Y, Ali A. Matrix type transdermal drug delivery systems of Metoprolol Tartrate: in vitro characterization. *Acta Pharm.* 2003 Jun 1;53(2):119-26.
13. Cho CW, Shin SC. Enhanced transdermal delivery of Atenolol from the ethylene vinyl acetate matrix. *Int J Pharm.* 2004 Dec 9;287(1-2):67-71.
14. Limpongsa E, Umprayn K. Preparation and evaluation of Diltiazem Hydrochloride diffusion-controlled transdermal delivery system. *AAPS PharmSciTech.* 2008 Jun; 9:464 70.
15. Ren C, Fang L, Li T, Wang M, Zhao L, He Z. Effect of permeation enhancers and organic acids on the skin permeation of indapamide. *Int J Pharm.* 2008 Feb 28;350(1-2):43-7.
16. Murthy SN, Hiremath D. Transdermal drug delivery systems. In: *Textbook of industrial pharmacy.* Hyderabad: Orient Longman Private Limited; 2008. p. 27-49.
17. Arunachalam A, Karthikeyan M, Kumar DV, Prathap M, Sethuraman S, Ashutoshkumar S, et al. Transdermal drug delivery system: a review. *J Curr Pharm Res.* 2010 Oct 1;1(1):70.
19. Praveen Tyle. Drug delivery device fundamental and biomedical application. Marcel Dekker, New York. 1988; 386-419.
18. Remington's Pharmaceutical Science. 17th ed. Mack Publishing Co. 1995; 1644-1661.
19. Bellantone NH, Rim S, Rasadi B. Enhanced percutaneous absorption via Iontophoresis I. Evaluation of an in-vitro system & transport of model compound. *Int J Pharm.* 1986; 30: 63-72.
20. Gros L, Clark WE. The structure of skin" in "The tissue of the body. Le Gros & Clark W. E.(editors) edition VI, ELBS and Oxford University Press, London. 1980; 29-313.
21. Saxena M, Mutualik S, Reddy MS. Formulation and evaluation of transdermal patches of Metoclopramide Hydrochloride. *Indian drugs.* 2006;43(9):740-5.
22. Darwhekar G, Jain DK, Patidar VK. Formulation and evaluation of transdermal drug delivery system of Clopidogrel Bisulfate. *Asian J. Pharm. Life Sci.* ISSN. 2011; 2231:4423.
25. Bhatia C, Sachdeva M, Bajpai M. Formulation and evaluation of transdermal patch of Pregabalin. *Int. J. Pharm. Sci. Res.* 2012 Feb 1; 3(2):569.
23. R Madan J, S Argade N, Dua K. Formulation and evaluation of transdermal patches of systemic agents. *J Pharm Res.* 2007 Apr;6(2):44-50.

donepezil. Recent patents on drug delivery & formulation. 2015 Apr 1; 9(1):95-103.

HOW TO CITE: Suhas B. C., Nagendra R.*, Siddartha H. N., Venkatesh, Hanumanthachar Joshi, Formulation and Evaluation of Transdermal Patches Containing Astragaloside IV, *Int. J. of Pharm. Sci.*, 2025, Vol 3, Issue 10, 2828-2847
<https://doi.org/10.5281/zenodo.17452263>

